Oleoresin Chemistry and Spectral Reflectance in "Stressed" Lodgepole and White Bark Pine, Mammoth Mountain, California

James C. Hickey,[1] Richard W. Birnie,[1] Meixun Zhao[1]

I. Introduction/Background

Development of methods to identify the physical and chemical character of materials on the earth's surface is one of the foci of hyperspectral remote sensing activities. Enhancing the ability to elucidate changes in foliar chemistry that relate to the health of a plant is a benefit to plant physiologists, foresters, and plant ecologists, as well as geologist and environmental scientists. Vegetation covers the landscape throughout the temperate and tropical regions of the earth. The existence of vegetation in these areas presents special problems to remote sensing systems since geologic bedrock and alteration zones are masked (Sabins, 1999). At times, however, alterations in the soil/sediment geochemical environment result in foliar chemical changes that are detectable via remote sensing. Examples include monitoring of chlorophyll reflectance/fluorescence and equivalent water thickness indices as indicators of drought-induced plant stress (Datts, 1999; Zarco-Tejada, et al. 2000). Another processing and interpretation approach used with hyperspectral data has been principal components analysis (PCA). Rowan, et al. (2000), used PCA to identify absorption feature patterns obtained from vegetated areas with discrete bedrock geology or mineralization as the substrate. Many researchers highlight the need to advance our ability for hyperspectral imaging in vegetated areas as a near-term priority (Vincent, 1997 and Sabins, 1999).

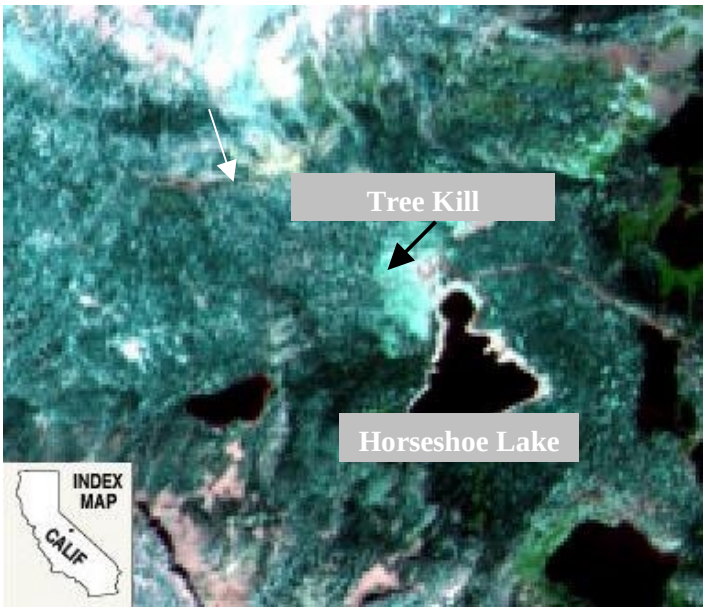

Figure 1. AVIRIS image of Horseshoe Lake and tree kill area. Bright area immediately southwest of the lake is the closed USFS campground and high CO_2/tree kill area. This scene was extracted from 1999 JPL AVIRIS Flight Line over Mammoth Mountain.

The premise of this investigation is to elucidate the connection between changing geochemical substrates (high [CO_2] in soil gas], resultant changes in conifer biochemistry (i.e., monoterpenes in oleoresin and other coincidentally responding constituents) and any associated alteration of the plant's reflectance curve. Predicting a change in monoterpene/oleoresin chemistry and in turn the geochemical substrate, using either field spectroscopy or hyperspectral imagery, is the ultimate goal of the research behind this project.

1 – Dartmouth College, Department of Earth Sciences; jhickey@dartmouth.edu

A preliminary sampling program was conducted in October 2000 at the Horseshoe Lake (HSL) tree kill area, Mammoth Mountain, California (Figure 1). The HSL tree kill is situated on the north and west sides of Horseshoe Lake. Conifers dominate the HSL area with lodgepole (*Pinus contorta)* and white bark (*Pinus albicaulis*) pines being the most common species identified and sampled during this study.

Mammoth Mountain is a cumulovolcano that was formed as a result of multiple eruptions from more than 10 different edifices 100,000 to 300,000 years ago (Sorey, et al. 1998). It is located in the eastern Sierra Mountains on the southwest corner of Long Valley Caldera. Increased magmatic activity occurred in the late 1980's across the western portion of the caldera (Sorey, et al. 1998). This magmatic activity was indicated by increases in seismicity, expansion of the caldera's resurgent dome and higher levels of fumarolic activity (Sorey, et al. 1998). Initiation of diffuse CO_2 discharge at several locations around the mountain occurred in late 1989 (Sorey, et al. 1998). The source of the CO_2 is interpreted to be a subsurface reservoir of magmatically derived CO_2 that was breached (Farrar, et al. 1995 and Sorey, et al. 1998) as a result of the deformation. It is theorized that the excessive concentrations of CO_2 (> 50%) in the soil gas may have decreased root function of the trees in these areas (Farrar, et al. 1995). A decline of tree health that eventually leading to tree kills in the area of highest CO_2 concentration (see Figure 2) then followed (Farrar, et al. 1995). Though the area of the HSL tree kill has remained relatively constant for the last three to four years, trees forming the periphery of the main kill area still display indications of health impact (e.g., needle loss or >35 % of dead/dying branches).

Figure 2. View of the Horseshoe Lake tree kill from the former campground parking lot.

The HSL tree kill area has been the target of multiple geochemical and remote sensing studies since its discovery in 1994. Members of the USGS Volcanic Hazard Monitoring team have been collecting CO_2 soil gas and flux data since 1994 (Farrar, et al. 1995). The status of tree health and detection of the CO_2 boundary temporal shifts were investigated by DeJong (1996), Hausback, et al. (1998) and Martini, et al. (2000) using a combination of field spectroscopy, AVIRIS and other hyperspectral imagery. Since conifers of varying health are still present around the boundary area, HSL was selected to test our premise. One objective of this ongoing investigation is to elucidate the connection between changing geochemical substrates, resultant changes in conifer biochemistry (i.e., monoterpenes in oleoresin or other coincidentally respondent constituents) and any associated alteration of the plant's reflectance spectrum. Predicting a change in monoterpene/oleoresin chemistry and in turn the nature of the geochemical substrate, using either field spectroscopy or hyperspectral imagery, is the ultimate goal of this research.

Soil vapor surveys conducted for resource exploration and environmental investigations first indicated the connection between alterations in monoterpene chemistry and changing geochemical substrates. The presence of sesquiterpenes (the C_{15} terpenoids) was found to indicate the presence of fault and fracture systems in several soil vapor surveys (Hickey, et al. 1983 and Hickey, 1986). Additionally, previous commercial soil vapor data also indicated that organic vapor samples collected from conifers growing on geochemically normal and anomalous substrates contained different ratios of monoterpenes

(Hickey, unpublished data). These observations support the premise that a discernable relationship exists between changes geochemical substrate and coincident changes in oleoresin/monoterpene chemistry.

Oleoresin is a secondary metabolic product in conifers that is used as a plant defense agent (Gijzen, et al. 1993 and Taiz, L. and Zeiger, C., 1998). It consists of approximately 50% monoterpenes and 50% diterpane resin acids and exists in resin ducts and specialized cells that are distributed throughout the trunk, branches, twigs and needles of conifers (Gijzen, et al. 1993 and Litvak and Monson, 1998). Since the monoterpenes are indicative of oleoresin chemistry, they were selected as the proxy to measure the oleoresin changes. Monoterpenes found in conifers are C_{10} olefinic hydrocarbons that are synthesized for plant defense purposes (Gijzen, et al. 1993 and Litvak and Monson, 1998). The monoterpenes consist of over 20 different compounds and optical isomers. Many plant physiologists report variations of monoterpene chemistry as a function of decreasing plant health and different types of impact (e.g., herbivory versus alleopathy or drought versus increasing [CO_2]) indicating that monoterpene chemistry is sensitive to environmental change (Gijzen, et al. 1993 and Litvak and Monson, 1998). Biotic impacts typically induce more drastic compositional changes than abiotic impacts (e.g., 10 fold increase of 3-carene during bark beetle infestation where only 0.5 fold increase of a-pinene when atmospheric CO_2 is increased) (Gijzen, et al. 1993).

Previous researchers have demonstrated that many organic chemicals found in the foliage and branches of trees and shrubs are active in the NIR portion of this spectral range (Elvidge, 1990, Bammel and Birnie, 1994, Kokaly and Clark, 1999). The spectral activity in this region is associated with a series of combination and overtone bands derived from organic compounds with fundamental vibrations around 3000 to 5000 nm (the mid infrared or MIR). The IR absorption features typically found in this region area associated with vibrational modes of C-H, O-H and C-O bonds in the molecules (Weyer, 1985 and Workman, 1996). It should be noted that each of the monoterpenes have slightly different absorption features in the MIR (Weyer, 1985 and Workman, 1996) and by inference, in the NIR.

Elvidge (1990) analyzed various plants and associated biochemical materials by VNIR reflectance spectroscopy to identify the primary absorption features. Of particular interest to this study was the series of spectra recorded from the bark, needles and cones of pinion pine at three levels of dehydration (Elvidge, 1990). A sample of oleoresin (sap) was also analyzed as part of the pinion pine analytical suite evaluated by Elvidge (1990). Elvidge (1990) identified a series of absorption features from the pinion sap. These features occurred at 860, 910, 990, 1140, 1190, 1450, 1670 and 1930 nm, the majority of which correspond to C-H bond types that are prevalent in monoterpenes.

Hyperspectral imaging systems collect EM energy in the range of 350 to 2500 nm (visible-near infrared or VNIR) with significantly narrower bandwidths than other remote sensing systems. In the case of the AVIRIS system, the spectral bandwidth is 10 nm resulting in the acquisition of high-resolution spectral signatures from 20 m^2 scene pixels (Green, et al. 1998). Another objective of this research is to apply prominent absorption features elucidated above to the AVIRIS imagery of Mammoth Mountain.

II. Field and Laboratory Methods

Twig and needle samples representing the last two to three growth seasons were collected from lodgepole (*Pinus contorta*) and white bark (*Pinus albicaulis*) pines throughout the HSL tree kill site in October 2000. Using a visual needle retention index, tree specimens were classified as healthy, one of three stages of declining health and dying/dead. The health classes were based on visual observations of needle retention and percent of dead branches throughout the crown. Though the five different classes are clearly separated in many of the samples, approximately 30% of the healthy/slight impact and moderate/heavy impact samples show significant overlap. This indicates that there are likely only three and a maximum of four classes that can be distinguished. Future sampling efforts will evaluate this observation.

Sample collection involved clipping twigs and needles from branches at the top of the lower third of the canopy to minimize shading differences. After clipping the samples, they were placed in Ziplock© freezer bag with a damp paper towel and stored on ice then transported back to a temporary field lab for spectral analysis. A sub-sample of the twigs and needles were also placed in 20 ml VOA vials with

Teflon©-lined caps, stored on ice and transported to the organic geochemistry laboratory at Dartmouth College for monoterpene analysis.

A temporary field laboratory was established using a table, light stands and tripod for analytical consistency. The samples were analyzed using an ASD© Field Spec VNIR spectrometer in a fixed position at a height of 0.75 meters above the table/light stand setup. The spectrometer collects EM energy at the fiber-optic detector in the spectral range of 350 to 2500 nm and spectral resolution of 10 nm (ASD). The spectrometer is controlled using an on-board PC notebook computer that collects, stores and allows initial data processing/reformatting. Replicate samples were collected in reflectance mode after calibrating the spectrometer to a white reference standard. Example VNIR reflectance spectra for each health class are provided in Figure 3.

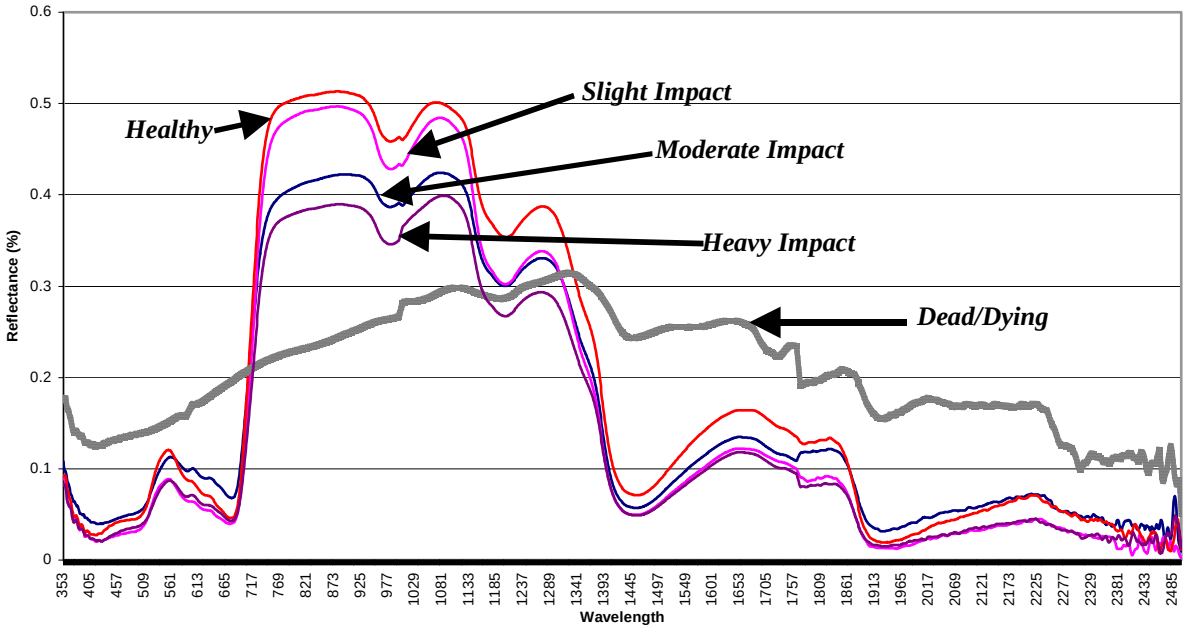

Figure 3. Reflectance spectra of lodgepole pine (*Pinus contorta*) from Horseshoe Lake tree kill area. Reflectance curves represent a series of samples showing declining health as determined by needle retention and percentage of dead branches across entire canopy.

Monoterpene compositions of the different specimens were measured by headspacing pine needles using Solid Phase Micro-extraction (SPME) field sampler manufactured by Supelco©. The SPME sampler consists of a retractable tippet comprised of 100 µms of PDMS absorbent coated on an inert substrate that was developed by Pawlisyn (1999). Preparation of the needles involved slicing the full needles into ~1cm lengths, transferring the particles into a pre-cleaned 40 ml VOA vial, adding 10 µls of a solution of 1,9 decadiene in $MeCl_2$ as an internal standard. After a one-minute exposure to the sample headspace, the SPME sampler was desorbed in the GC inlet directly onto the analytical column. The GC system included an HP© 6890 GC with a manual injector and SPME liner running isothermally at 250°C in a 100:1 split mode. The GC system also included a 50m HP-1 column operated with a programmed temperature mode of 40°C with an initial ramp of 4°C/minute to 220°C and a 2 minute hold time then 20°C/minute to a final temperature of 300°C and an FID running isothermally at 320°C. The data were acquired and preprocessed using HP© Chemstation© software. Identification of the compounds was performed using retention time database for the monoterpenes previously established in our lab. Monoterpene concentrations were calculated using the internal standard/compound peak areas, internal standard concentration and a single point calibration algorithm.

Each dataset was evaluated independently to facilitate feature selection and investigate any variance as a function of apparent plant health. An overview of the processing steps employed is shown in Figure 4. After the pertinent features were selected from each set, the covariance between the monoterpenes and spectral features was evaluated using ANOVA and regression techniques.

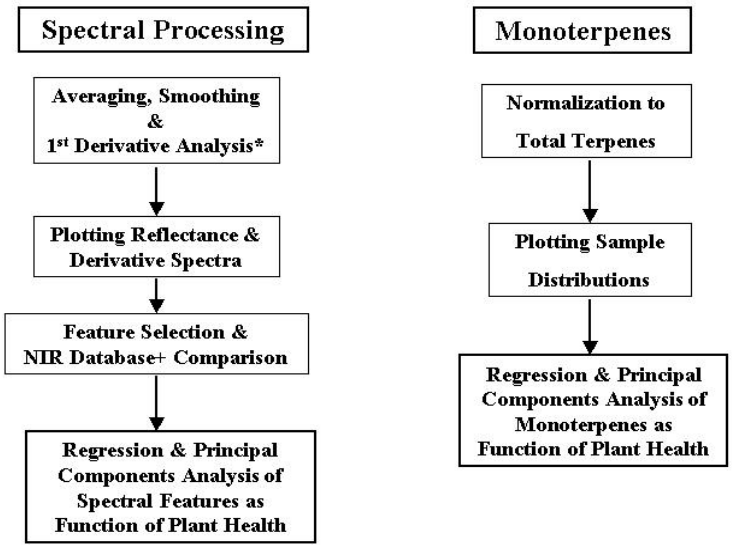

Figure 4. Flowcharts of processing steps used in evaluation of monoterpene (oleoresin) & spectral absorption features

III. Results and Discussion

The reflectance spectra depicted in Figure 3 shows there is an obvious decrease in NIR reflectance with decrease in tree health. Further data processing and interpretation was undertaken to identify prominent absorption features. Identification of absorption peak shifts involved interpretation of the 1st derivative transformation of the reflectance spectra (Tsai and Philpot, 1998). Examples of the 1st derivative curves are shown in Figure 5. Table 1 compares the key absorption peaks in our study with those of pinion oleoresin (Elvidge 1990). It is clear that, though the peaks do not coincide exactly, they fall in close proximity to each other. The differences are attributed to the variation in the plant biochemistry as a function of health.

Many of the characteristic absorption features found in the pure compounds are close to the features we identified. The oleoresin monoterpenes, however, are a mixture of eight or more compounds (Hirschfeld, T., & Hed, A. Z., (1981)). Any reflectance spectra derived from the oleoresin/monoterpenes, therefore, represent a combination of the individual constituent spectra. Since pines of different health levels have different monoterpene compositions, each mixture is expected to have different NIR signals and slight shifts in band position are expected. Additionally, the bond types associated with absorption features reported in Table 1 are derived from C-H bond variations prevalent in monoterpenes. It is important to note that other organics (e.g., sugars, waxes, etc.) also contain similar bonds. Further work is required to increase our understanding of the absorption feature source before a direct correlation between the absorption features and oleoresin/monoterpenes can be established.

TABLE 1: Pertinent Absorption Feature Comparison (nm)

ELVIDGE, 1990	**-**	**860**	**910**	**990**	**1140**	**1190**	**-**	**1450**	**1670**	**-**	**1920**
CURRENT	**670**	**880**	**-**	**980**	**1075**	**1200**	**1270**	**1450**	**1650**	**1820**	**1920**

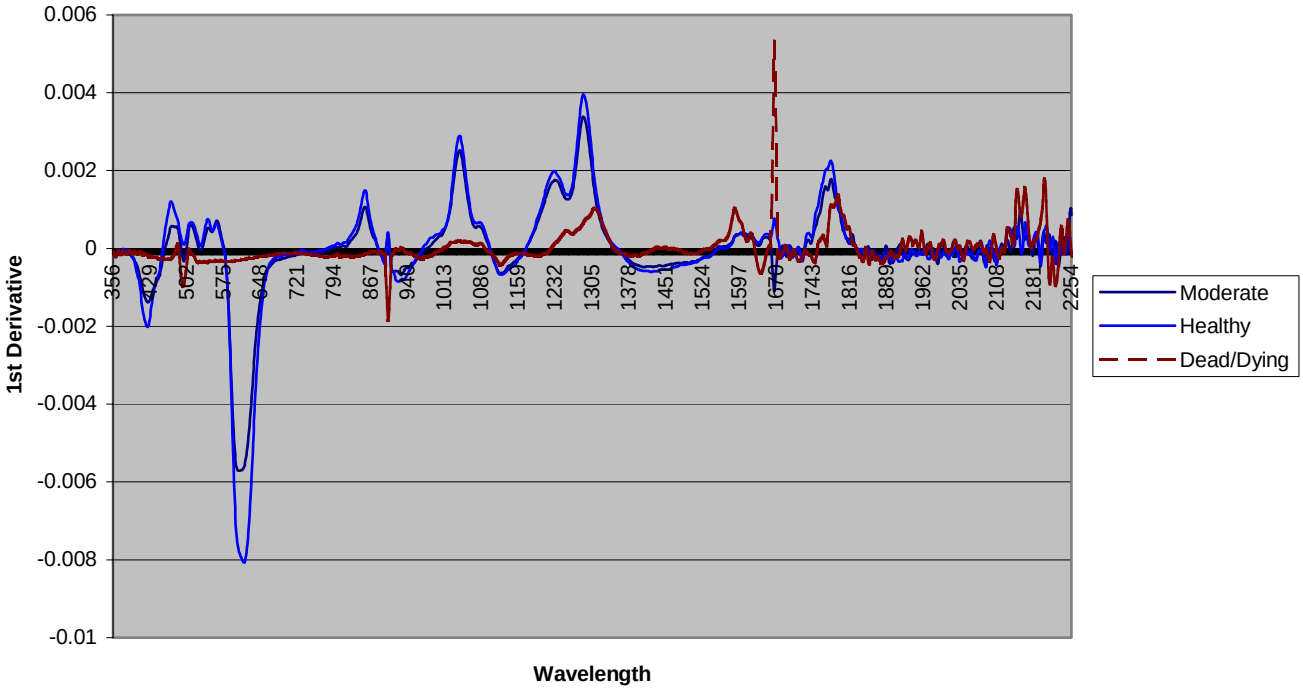

Figure 5. 1st derivative spectra from Horseshoe Lake lodgepole pine sample. Examples are the same samples used to create Figure 3 (reflectance spectra).

A combination of bivariate plot analysis, ANOVA and regression techniques was employed to assess the ability of the features listed in Table 1 for separating healthy from dying/dead pines. The features at 670, 880, 980, 1450, 1650, 1820 and 1920 nm separated the samples into two clusters. The intermediate health class samples (distinct signs of impact and with < 65% intact branches) tended to cluster around the healthy samples relative to the absorption features above 1450 nm. A greater level of dispersion, especially of the samples approaching greater than 35% intact branches, was observed in the shorter wavelength features. The features at the longer wavelengths are likely related to water loss. It is clear that some of the features (980, 1200, 1450 nm) fall in close proximity water absorption bonds, but the others do not. As a plant's health declines, many biochemicals, such as the monoterpenes, go through both a compositional change and quantitative reduction, as the plant re-allocates its energy and carbon resources.

Evaluation of the monoterpene chemistry was conducted to identify general trends in the composition relative to tree health. First, a few similarities and differences are observed when comparing the relative quantities of monoterpenes from the lodgepole and white bark pines. Where beta-pinene (50 to 75%), alpha-pinene (9 to 15%) and limonene (8 to 28%) are the most prominent terpenes in lodgepole pine, 3-carene (40 to 70%), alpha-pinene (12 to 25%) and myrcene (5 to 20%) dominate the composition of white bark pine. A graphical depiction of the composition for the lodgepole pine end-members is provided in Figure 6. Examples of monoterpene chemistry alteration related to possible biotic influences were also observed. In the case of lodgepole pine, the relative concentrations of alpha and beta pinene decreased where 3-carene and terpinolene increased in samples indicating biotic impacts. Nearly the opposite occurred in white bark pine. Alpha pinene and myrcene were all found to increase while phellandrene, terpinene and terpinolene decreased in relative concentration. Similar but subtler results were observed in the absolute monoterpene concentration data. The influence of both biotic and abiotic impact leads to a

higher level of complexity in the intermediate health classes. Identification and separation of the abiotic and biotic influences is, therefore important. Data processing and interpretation is continuing in this regard.

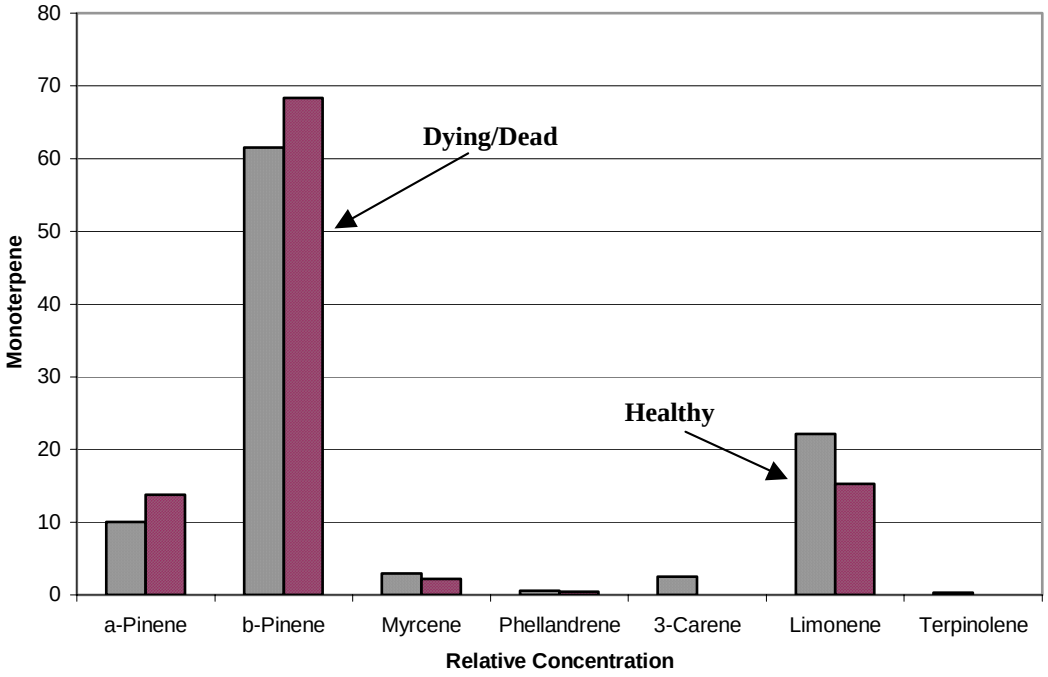

Figure 6. Example relative concentration change for the healthy (medium gray) and dying/dead (dark gray) lodgepole pine samples.

After evaluating each of the variables independently, we investigated the variables pair-wise to identify any significant co-varying sets that separate the end-member classes. Bivariate scattergrams for the reflectance value of each prominent absorption feature versus the relative concentration of each of monoterpenes were prepared. Table 2 summarizes all of the pairs that both discriminate the healthy from dying/dead clusters and indicate the presence of a statistically significant linear regression fit. A graphical example of the regression analyses depicting a positive correlation is provided in Figure 7. Superposition of the remaining "intermediate health" samples onto the regression models indicates there are multiple influences that lead to a high degree of variance in the data. An example of this is the biotic versus abiotic influences on monoterpene response. Attempts to mathematically resolve these complexities using techniques such as principal components and discriminant analyses are ongoing.

Table 2: Results of Covariance Analysis for Monoterpene-Absorption Feature Pairs of Lodgepole Pine End-members

SPECTRAL BAND	MONOTERPENE	R	R^2	F RATIO	PROB>F
670 nm	Alpha-pinene	0.67	0.45	9.1	0.012
880 nm	Alpha-pinene	0.75	0.57	14.5	0.003
1450 nm	Alpha-pinene	0.82	0.67	22.7	0.001
1820 nm	Alpha-pinene	0.83	0.70	25.1	0.0004
1920nm	Alpha-pinene	0.85	0.72	27.9	0.0003
1650 nm	Beta-pinene	0.81	0.66	23.3	0.0004
880 nm	Limonene	0.78	0.62	17.7	0.002
980 nm	Limonene	0.71	0.5	11.0	0.007
1075 nm	Limonene	0.66	0.44	8.5	0.013
1650 nm	Limonene	0.73	0.53	13.4	0.003

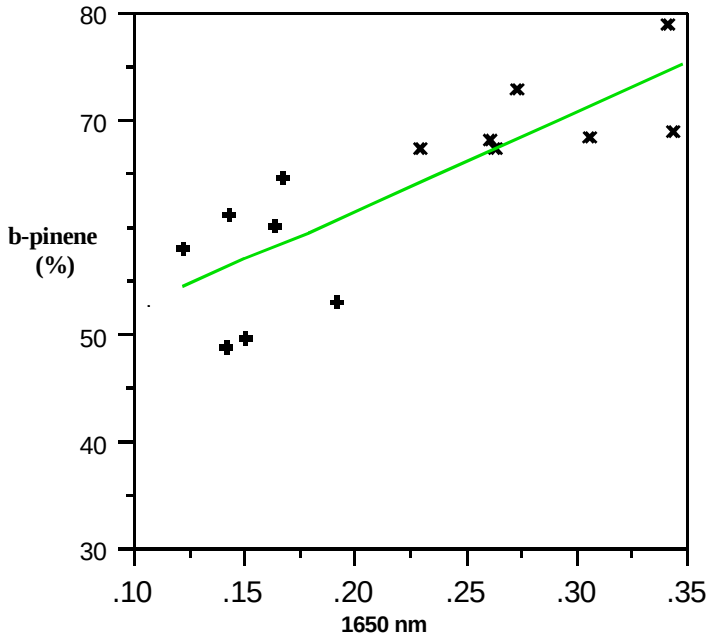

Figure 7. Regression results where the intensity of the absorption band at 1650 nm is plotted vs. the relative concentration of beta-pinene. The + markers correspond to the healthy samples and the x markers to the dying/dead samples of lodgepole pine.

Efforts to date have focused on elucidating the monoterpene-field spectroscopic relationship. Initial processing (atmospheric correction) of the AVIRIS 1999 Mammoth Mountain flight line data is currently underway. Once completed, use of the absorption features identified to assist in image interpretation will commence.

IV. Summary and Future Efforts

Sampling and analysis of lodgepole white bark pines to evaluate the relationship between oleoresin chemistry and spectral reflectance changes as a function of plant health were completed at the HSL tree kill area, Mammoth Mountain, California during the Fall of 2000. Both review of the literature and the analysis of our HSL dataset indicate that each variable undergoes a series of changes that relate not

only to the health state but also the nature of the impact (i.e., biotic vs. abiotic). Included are the identification of a series of absorption features and monoterpene composition that discriminate between the two end-member health states (healthy vs. dying/dead). Additionally, covariance and regression analysis between the absorption features and monoterpenes shows that a statistically significant model exists that also separates the healthy from dying/dead end-members of the conifers.

This paper is summarizes the preliminary results of an ongoing study. The first phase of field and analytical work lead to several exciting and promising results and additional rounds of field sampling and data analysis will occur throughout 2001. The products of this work will be used to enhance both our understanding of the underlying biogeochemical-spectral relationships and how it may be applied to processing and interpreting the hyperspectral imagery for the area.

V. Acknowledgements

We wish to extend our sincere appreciation to the Dartmouth College, Department of Earth Sciences and NASA NH Space Grant Consortium for their continuing financial support of this research, Dr. Bert Davis (USCOE-CRREL) for the use of their ASD Field Spectrometer, Dr. Barry Rock (UNH-Complex Systems) and Dr. David Pieri (NASA-JPL) for their insight of the field area, and lastly, Dr. Michael Sorey (USGS) and Larry Ford (USFS) for their help with obtaining access to the research area.

VI. References

Analytical Spectral Devices, Field Spectroradiometer Manual

Bammel, B. H. & Birnie, R. W. (1994), Spectral reflectance response of big sagebrush to hydrocarbon-induced stress in Bighorn Basin, Wyoming, Photo. Eng. & Remote Sen., 60 (1), 87-96

Datts, B. (1999), Remote sensing of water content in Eucalyptus leaves, Austral. J. of Bot., 47(6):909-923

DeJong, S. M. (1996), Surveying dead trees and CO_2-induced stressed trees using AVIRIS in the Long Valley Caldera, in Sum. of the Sixth Ann. JPL Airb. Earth Sci. Wkshp, JPL Pub. 96:67-74

Elvidge, C. D. (1990), Visible and near infrared reflectance characteristics of dry plant materials. Int. Jour. of Remote Sensing, 11:1775-1795

Farrar, C. D., et al. (1995), Forest-killing diffuse CO_2 emissions at Mammoth Mountain as a sign of magmatic unrest. Nature, 376:675-677

Gijzen, M., et al. (1993), Conifer Monoterpenes: Biochemistry and Bark Beetle Ecology in Bioactive Volatile Compounds from Plants, American Chemical Society, Washington, D.C., 309 p.

Green, R. O., et al. (1998), Imaging spectroscopy and the airborne visible infrared imaging spectrometer (AVIRIS), Remote Sens. Environ., 65:227-248

Hausback, B. P., et al. (1998), Monitoring of volcanogenic CO_2-induced tree kills with AVIRIS image data at Mammoth Mountain, California, in Sum. of the Seventh Ann. JPL Airb. Earth Sci. Wkshp, JPL Pub. 98

Hickey, J. C., Klusman, R. W., Voorhees, K. J. (1983), Fault leakage characterization by integrative gas geochemistry/mass spectrometry/pattern recognition procedures, AAPG Bulletin, 67 (8), p. 1342

Hickey, J. C. (1986), Colorado School of Mines – Unpublished Master's Thesis no. T-3080, 72 p.

Hirschfeld, T., and Hed, A. Z. (1981), The Atlas of Near Infrared Spectra. Sadtler Res. Labs: Phil. PA

Kokaly, R. F. and Clark, R. N. (1999), Spectroscopic determination of leaf biochemistry using bad-depth analysis of absorption features and stepwise multiple linear regression. Rem. Sens. Of Envir., 67:267-287

Litvak, M. E., and Monson, R. K. (1998), Patterns of induced and constitutive monoterpene production in conifer needles in response to herbivory, Oecologia, 114:531-540

Martini, B. A., et al. (2000), Geological and Geobotanical Studies of Long Valley Cladera, CA, USA, utilizing new 5mm hyperspectral imagery, *Proc. IEEE Int'l. Geosc./Remote Sensing Symp.* July 2000

Pawlisyn, J. (1997), Solid Phase Microextraction – Theory and Practice Wiley-VCH, NY, 246 p.

Rowan, et al. (2000), Mapping hydrothermally altered rocks by analyzing hyperspectral image (AVIRIS) data of forested areas in the southeastern United States, J. Geoch. Expl., 68(3):145-166

Sabins, F. F. (1999), Remote sensing for mineral exploration, Ore Geol. Rev., 14:157-183

Sorey, M. L., et al. (1998), Carbon dioxide and helium emissions from a reservoir of magmatic gas beneath Mammoth Mountain, California. Jour. of Geophys. Res., 103:15303-15323

Taiz, L. & Zeiger, C. (1998), Plant Physiology, Sinauer Assoc., Inc., Sunderland, MA, 792 p.

Tsai, F. and Philpot, W. (1998), Derivative analysis of hyperspectral data, Rem. Sens. Environ., 66:41-51

Vincent, R. K. (1997), Fundamentals of Geologic and Environmental Remote Sensing, Prentice Hall, Upper Saddle River, NJ 366 p.

Weyer, L.G., (1985), Near-Infrared Spectroscopy of Organic Substances, Appl. Spec. Rev. 21(1&2):1-43

Workman, J. J., (1996), Interpretative Spectroscopy for Near Infrared, Appl. Spec. Rev., 31(3):251-320

Zarco-Tejada, P. J., et al. (2000), Chlorophyll fluorescence effects on vegetation apparent reflectance: II. Laboratory and airborne canopy-level measurements with hyperspectral data, Remote Sens. Environ. 47:596-605